Arch Toxicol (2001) 75: 425–438
DOI 10.1007/s002040100251

ORGAN TOXICITY AND MECHANISMS

Jeffrey R. Haskins · Paul Rowse · Ramin Rahbari
Felix A. de la Iglesia

Thiazolidinedione toxicity to isolated hepatocytes revealed by coherent multiprobe fluorescence microscopy and correlated with multiparameter flow cytometry of peripheral leukocytes

Received: 21 March 2001 / Accepted: 29 May 2001 / Published online: 1 August 2001

Abstract Thiazolidinediones (TZDs) are effective for the treatment of adult-onset insulin-resistant diabetes. Unfortunately, TZDs are associated with sporadic hepatic dysfunction that is not predictable from experimental animal studies. We investigated the response of isolated rat and human hepatocytes to various TZDs using biochemical assays, coherent multiprobe fluorescence microscopy and flow cytometric analyses. The results identified direct effects of TZD on mitochondria from live human and rodent hepatocytes. The multiprobe fluorescence assays showed disruption of mitochondrial activity as an initiating event followed by increased membrane permeability, calcium influx and nuclear condensation. Other TZD-related cellular effects were increased hepatic enzyme leakage, decreased reductive metabolism and cytoplasmic adenosine triphosphate depletion. Mitochondrial effects were similar in cryopreserved hepatocytes from diabetic or non-diabetic donors. Peripheral blood mononuclear cells (PBMCs) had baseline mitochondrial energetics and metabolism comparable with isolated hepatocytes. Mitochondrial effects in isolated hepatocytes were found in human PBMCs exposed to the TZDs. The relative potency of TZDs for causing hepatocyte and PBMC effects was troglitazone > pioglitazone > rosiglitazone. These studies clearly demonstrated that hepatic alterations in vitro are characteristic of TZDs, with only quantitative differences in subcellular organelle dysfunction. Monitoring mitochondrial function in isolated PBMCs may be beneficial in diabetics undergoing TZD therapy.

Keywords Thiazolidinediones · Peripheral leukocytes · In vitro · Comparative toxicity · Liver

J.R. Haskins · P. Rowse · R. Rahbari
Drug Safety Evaluation,
Pfizer Global Research and Development,
Ann Arbor, Michigan 48105, USA

F.A. de la Iglesia (✉)
Department of Pathology,
The University of Michigan Medical School,
7520 A MSRB-I, 1150 W Medical Center Drive,
Ann Arbor, Michigan 48109, USA
E-mail: felixdelaiglesia@provide.net
Tel.: +1-734-6472937
Fax: +1-734-7691504

Introduction

Thiazolidinediones (TZDs) comprise a group of drugs for the treatment of adult-onset insulin-resistant diabetes that increase insulin sensitivity, improve glucose control, and lower glycosylated hemoglobin 1 A, serum triglycerides and circulating insulin (Fonseca et al. 1998; Iwamoto et al. 1991; Saltiel and Olefsky 1996; Schwartz et al. 1998). In animal models of diabetes, including ob/ob, K/K and db/db mice and Zucker fatty rats, TZDs reduced plasma glucose, insulin levels, ketone bodies, triglycerides and plasma lactate (Fujiwara et al. 1988). The mechanisms by which cellular metabolic changes take place in diabetics are not fully understood, and glitazones activate the peroxisome proliferator-activated receptor γ (PPARγ) and modulate hepatic glucose transport, improve glucose utilization in skeletal muscle and cause pre-adipocyte differentiation (Lehmann et al. 1995). TZDs have been used effectively in a large number of diabetics, who, as a result, experienced significant reduction of insulin requirements (Fonseca et al. 1998; Iwamoto et al. 1991; Schwartz et al. 1998). However, one compound in this class, troglitazone (see Fig. 1) caused sporadic hepatic dysfunction and hepatic failure in a number of cases (Watkins and Whitcomb 1998). These reactions were not predictable from standard toxicological models (de la Iglesia et al. 1998; Herman et al. 1997, 1998; McGuire et al. 1997, 1998; Rothwell et al. 1997; M.M. Shi, M.R. Bleavins, R.G. Thompson, J.F. Chin and F.A. de la Iglesia, submitted for publication).

From the literature it is not possible to determine if these idiosyncratic reactions were due to altered biotransformation or conjugation mechanisms, a susceptible

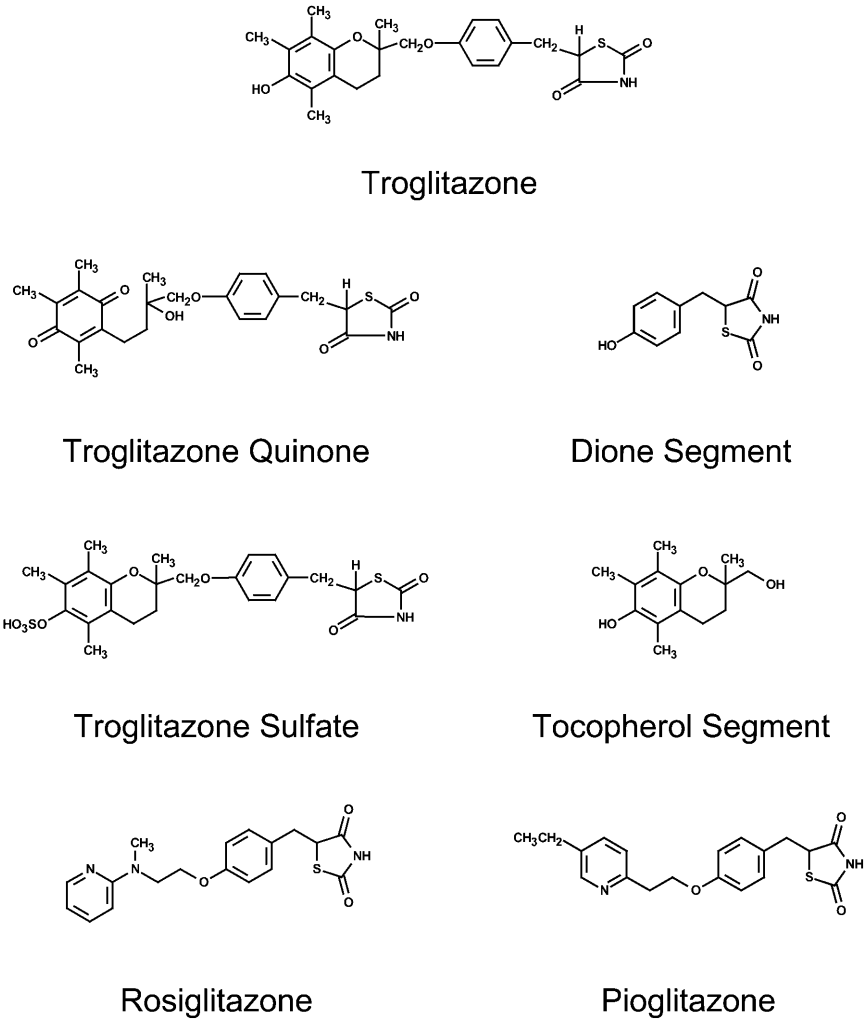

Fig. 1 Structure of thiazolidinediones, related compounds and metabolites used in these studies

genotype, damaging drug metabolism interactions within the liver cell, or to decreased hepatic function as a result of pre-existing diabetic pathology (Cabarrou et al. 1973; Murakami and Shima 1995; Silverman et al. 1989). Frequently, type II diabetics receive different concomitant medications for glucose control, hypertension, arthritis, pain and hypercholesterolemia (Tattersall 1995). Compromised hepatic lipid or carbohydrate metabolism is not easily assessed in diabetics under current clinical laboratory protocols. These underlying diabetic alterations in the liver depend on advancing age, sex or coexisting pathology, such as hepatitis B or C, chronic cholestasis or alcoholism (Silverman et al. 1989).

The effects of TZDs on human or animal live isolated hepatocytes have not been explored in detail. Mitochondria from diabetic Zucker rats lack the ability to compensate for chemically induced uncoupling of oxidative phosphorylation (Haskins et al. 1999). To study the response of liver cell functions to pioglitazone, troglitazone and rosiglitazone, coherent multiprobe fluorescence assays have been used to determine time and dose relationships for decreased mitochondrial energetics, loss of plasma membrane integrity and altered calcium transport (Monteith et al. 1998; Plymale and de la Iglesia 1999; Plymale et al. 1999). The multiprobe fluorescence microscopy studies were followed by multiparameter flow cytometry in order to dissect the intracellular effects of TZDs on hepatocytes and peripheral blood mononuclear cells (PBMCs). Mitochondrial energetics, sulfation and glucuronidation are functions amenable for study in white blood cells or hepatocytes and have been explored with other drugs (Lowis and Oakey 1996). Thus, flow cytometric evaluation of PBMCs from diabetics taking TDZ medication would constitute a minimally invasive, accurate and sensitive assay at a moderate cost together with the benefit of predicting or preventing serious hepatic reactions.

Materials and methods

Hepatocyte isolation

Hepatocytes were isolated from 75- to 96-day-old female Wistar rats according to established methods with slight modifications (Deschenes et al. 1980; Seglen 1976). Hepatocytes, purified by differential centrifugation through a Percoll gradient, were washed and suspended in Liebowitz L-15 hepatocyte culture media (Gibco

BRL, Grand Island, N.Y., USA), supplemented with 7.5% bovine serum albumin, 1% penicillin/streptomycin, 3 mg/ml proline, 50 mg/ml galactose, 0.1% insulin-transferrin-selectin (Collaborative Biomedical Products, Bedford, Mass., USA), 0.4 mg/ml dexamethasone (Sigma, St. Louis, Mo., USA), 8.4% sodium bicarbonate and 0.1% trace elements. Viability of hepatocytes was assessed by Trypan blue exclusion. Plating was approximately 25,000 cells/well on 96-well collagen-coated plates and kept overnight at 37°C in a humidified 5% CO_2 incubator for the assessment of enzyme leakage, and dimethylthiazol diphenyl tetrazolium (MTT) and adenosine triphosphate (ATP) assays. For coherent multiprobe fluorescence microscopy, hepatocytes were plated at the same density on collagen-coated 8-chambered coverglasses (Nagle Nunc, Napervile, Ill., USA). Flow cytometry employed rat hepatocytes isolated as described above and normal or diabetic human hepatocytes obtained from In Vitro Technologies (Baltimore, Md., USA). Human and rat hepatocytes were suspended in Liebowitz media containing 5 μg/ml Hoechst 33342 and 100 nM tetramethylrhodamine ethyl ester (TMRE; Molecular Probes, Eugene, Ore., USA) and incubated for 25 min at 37°C in a humidified 5% CO_2-air interface prior to use. Incubation times, probe concentrations, and phototoxicity and photodegradation profiles were optimized for flow cytometry or fluorescence microscopy in preliminary experiments (data not shown).

Peripheral blood mononuclear cell isolation

Blood was collected from healthy volunteers and the red cells lysed in buffer (150 mM NH_4Cl, 1 mM EDTA and 10 mM $NaHCO_3$ (Sigma) for 10 min at room temperature. PBMCs were isolated after centrifugation at 300 *g* for 5 min and then suspended in RPMI-1640 media (StemCell Technologies, Inc., Vancouver, B.C., Canada) supplemented with 5% fetal bovine serum under the same conditions and probe concentrations as for hepatocytes.

Chemicals

Troglitazone, the quinone and sulfate metabolites, the tocopherol nucleus and the dione functional group, and rosiglitazone were dissolved in dimethyl sulfoxide (DMSO; Sigma) at 100 mM. Pioglitazone was prepared at 25 mM. All compounds were of ≥95% purity. Appropriate dilutions were prepared from fresh stock solutions in Liebowitz or RPMI-1640 media. DMSO was reagent grade and the concentration did not exceed 0.06% in the preparations.

Selection criteria for in vitro concentration

The therapeutic concentration of troglitazone ranges from 1 to 2 μg/ml, equivalent to 2.25–4.5 μM; the drug is >99% protein bound and humans have significantly lower blood concentrations than animals. (Kawai et al. 1997; Ott et al. 1998; Shibukawa et al. 1995) Troglitazone or pioglitazone at 20 μM inhibited transcriptional activity in fibroblast differentiation assays in serum-free media (Ihara et al. 2001). Troglitazone caused protein synthesis inhibition at 35–50 μM under serum-free conditions in human hepatocytes, and had inhibitory effects in sulfation-deficient porcine hepatocytes beginning at 50 μM with 90% inhibition at 100 μM (Kostrubsky et al. 2000; Ramachandran et al. 1999). Troglitazone inhibited gene expression of phosphoenolpyruvate carboxykinase and induced PPARγ activation in hepatocytes and HepG2 cells at concentrations between 100 and 200 μM in serum-containing media (Davies et al. 1999a, 1999b). ATP-dependent uptake of Neutral red was reduced by 80% under serum-free conditions with either 100 μM troglitazone or 100 μM rosiglitazone (Elcock et al. 1999). Our preliminary experiments showed that troglitazone decreased mitochondrial transmembrane potential ($\Delta\Psi_m$) by 25% at 25 μM in serum-free conditions or at 300 μM in complete media, by 50% at 50 μM and 400 μM, and by 75% at ≥100 μM and ≥500 μM, respectively. Concentrations of ATP decreased by 80% with 225 μM troglitazone and by 60% with 450 μM rosiglitazone in serum supplemented systems. These data indicate that serum-free conditions will augment observed cellular responses and effects may appear at different concentrations. All assay conditions in this report include protein-supplemented cultures.

Enzyme leakage assays

Culture media with or without drug was added to triplicate plates and incubated for 2 h at 37°C. Each assay was repeated three times. Media and cell lysates were assayed for alanine aspartate aminotransferases (ALT), aspartate aminotransferases (AST) and lactic dehydrogenase (LDH) in a Vitros 750 XRC analyzer (Ortho Clinical Diagnostics, Raritan, N.J., USA).

MTT assay

Culture media with or without drug was added to plates and incubated for 2 h at 37°C and replaced with media containing MTT (0.5%) (Sigma). After an additional 2 h at 37°C, media was replaced with 100 μl of DMSO. Quadruplicate plates were read at 570 nm on a SpectraMax spectrophotometer (Molecular Dynamics, Sunnyvale, Calif., USA).

ATP assay

ATP concentrations were measured using a luciferin-luciferase assay (ATP Lite-M kit; Packard, Meridien, Conn., USA). Cells were lysed and mixed with the substrate solution for 2 min, placed in the dark for 10 min and relative light units measured on a MLX microtiter plate luminometer (Dynex Technologies, Chantilly, Va., USA).

Coherent multiprobe fluorescence microscopy

The coherent fluorophore system was designed to follow time-related changes in $\Delta\Psi_m$, intracellular Ca^{2+} traffic, plasma membrane permeability and nuclear cell morphology (Plymale et al. 1999). Cells were loaded with 100 nM tetramethylrhodamine methyl ester (TMRM), 4 U/ml BODIPY 650/665 Phalloidin, 2 μM Fluo-4 AM and 2 μg/ml Hoechst 33342 (Molecular Probes) in culture media for 30 min at 37°C. Media containing 4 U/ml BODIPY 650/665 Phalloidin and 2 μg/ml Hoechst 33342 was added after a brief wash. Four areas per well were selected for observation, based on TMRM fluorescence threshold and ensuring a minimum of 80% viable cells. Treatment was initiated by adding an equal volume of media containing a 2× concentration of drug, 4 U/ml BODIPY 650/665 Phalloidin and 2 μg/ml Hoechst 33342. Digital images of the selected areas were captured every 10 min over 2 h. After appropriate photobleaching and phototoxicity validation protocols assured system stability and acceptance, the sequential exposures at each of the 10-min intervals were 3.0, 0.5, 0.75 and 0.25 s for Bopidy 650/665 phalloidin, TMRM, Fluo-4 and Hoechst 33342, respectively. The microscope was fitted with a 100 W mercury lamp and 360/460, 480/535, 546/580 and 640/680 nm excitation/emission filters. A differential interference contrast (DIC) image was obtained together with each of the fluorescence image sequences to assess cell morphology. A high-resolution liquid-cooled charge-coupled device (CCD) was used to acquire over 2080 images over the 2-h period from each experiment. Average pixel intensities were calculated using the raw 12-bit image and applying an image analysis algorithm (Image Pro Plus, Media Cybernetics, Silver Springs, Md., USA).

Hepatocyte and PBMC flow cytometry

At the start of the experiment, equal volumes of media containing cells and media with 2× drug concentration were mixed and kept in a humidified 5% CO_2 incubator at 37°C. For probe loading, cells were suspended in supplemented Liebowitz medium containing 5 μg/ml Hoechst 33342 and 100 nM TMRE and incubated for

25 min at 37°C. Aliquots of 15,000 cells were taken at 15-min intervals over 2 h and analyzed in an EPICS Elite flow cytometer (Beckman-Coulter, Miami, Fla., USA) with time-resolved 15-mW, 488-nm argon (upper) and 20-mW, 325-nm HeCd (lower) double excitation. Data collected from 15,000 cells were analyzed using WinList software (Verity Software, Topsham, Me., USA), which reported the number of cells with normal $\Delta\Psi_m$. Light scatter was used to identify lymphocytes, monocytes and granulocytes.

Statistical analysis

Differences between groups were determined by one-way analysis of variance (ANOVA) at a significance level of 5%. Supplemental analyses of rank-transformed data were used when necessary. Sigma Stat v.2.0 for Windows (SPSS, Chicago, Ill., USA) was employed for all statistical analyses.

Results

Enzyme leakage in isolated rat hepatocytes

Troglitazone at concentrations ≥400 μM caused LDH leakage of ≥3 times the background (Table 1). The sulfate and the quinone metabolite, the tocopherol nucleus or the dione functional group, and rosiglitazone did not cause significant enzyme leakage. ALT leakage of ≥2 times background was seen with troglitazone at ≥300 μM. The quinone metabolite at 600 μM caused a statistically non-significant 1.7-fold increase in ALT leakage, with no other significant increases found. At ≥400 μM, troglitazone caused 5.4- to 6.5-fold increases in AST leakage.

Reductive metabolism in isolated rat hepatocytes

Concentration-related decreases in reductive metabolism of MTT substrate was observed in troglitazone-treated rat hepatocytes. Reductive metabolism was similar to controls at 200 μM troglitazone, and decreased by 46%, 83%, 90%, and 89% at 300, 400, 500, and 600 μM, respectively (Table 2). The quinone metabolite produced no changes in reductive metabolism up to 400 μM, and decreased metabolism by 52% and 79% at 500 and 600 μM, respectively. The sulfate metabolite, the dione functional group or the tocopherol moiety did not cause changes in reductive metabolism at any of the concen-

Table 1 Enzyme leakage from isolated rat hepatocytes exposed to troglitazone and related compounds. Enzyme leakage (or extracellular enzyme activity) is expressed as percent of total enzyme activity (intracellular plus extracellular), mean ±SEM of three experiments (*LDH* lactic dehydrogenase, *ALT* alanine aspartate aminotransferase, *AST* aspartate aminotransferase, – data not available)

Compound	Concentration (μM)	Enzyme Leakage		
		LDH	ALT	AST
Control		27 ± 3	23 ± 5	12 ± 4
Troglitazone	200	20[a]	27 ± 2	13 ± 3
	300	17 ± 14	57 ± 2*	24 ± 3
	400	85 ± 1*	46 ± 7*	66 ± 6*
	500	88*[a]	53 ± 6*	79 ± *
	600	84*[a]	49 ± 5*	79 ± 3*
Troglitazone quinone	200	24 ± 1	34 ± 2	16 ± 3
	300	25 ± 2	33 ± 2	16 ± 4
	400	26 ± 1	34 ± 1	17 ± 3
	500	26 ± 1	29 ± 4	15 ± 1
	600	30 ± 2	40 ± 13	15 ± 2
Troglitazone sulfate	200	25 ± 2	29 ± 3	14 ± 2
	300	23 ± 2	29 ± 3	13 ± 2
	400	25 ± 2	32 ± 2	14 ± 3
	500	25 ± 2	32 ± 5	15 ± 2
	600	26 ± 2	34 ± 4	16 ± 3
Dione segment	200	23 ± 2	24 ± 4	13 ± 2
	300	23 ± 2	38 ± 16	–
	400	24 ± 3	26 ± 3	11 ± 1
	500	23 ± 2	27 ± 3	13 ± 2
	600	22 ± 2	28 ± 4	14 ± 2
Tocopherol segment	200	22 ± 3	24 ± 4	14 ± 3
	300	22 ± 3	27 ± 5	13 ± 2
	400	23 ± 3	26 ± 2	13 ± 3
	500	22 ± 1	25 ± 3	11 ± 2
	600	21 ± 1	25 ± 5	11 ± 3
Rosiglitazone	200	22 ± 2	26 ± 5	13 ± 1
	300	24 ± 2	24 ± 3	14 ± 2
	400	24 ± 2	30 ± 4	16 ± 2
	500	26 ± 2	28 ± 4	16 ± 2
	600	30 ± 4	27 ± 3	16 ± 1

[a] $n = 1$

*Statistically significant difference from control ($P < 0.05$)

Table 2 Reductive metabolism in isolated rat hepatocytes exposed to troglitazone and related compounds. Reductive metabolism is expressed as MTT [3-(4,5-dimethylthiazol-2-yl)-2,5-diphenyltetrazolium bromide] conversion in percent change from control values; mean ±SEM from four experiments

Compound	Concentration (μM)				
	200	300	400	500	600
Troglitazone	–12 ± 5	–46 ± 13*	–83 ± 10*	–90 ± 1*	–89 ± 1*
Troglitazone quinone	–4 ± 5	–12 ± 5	–14 ± 9	–52 ± 18*	–79 ± 13*
Troglitazone sulfate	–3 ± 6	–1 ± 11	–3 ± 10	–5 ± 7	–1 ± 6
Dione segment	13 ± 4	–3 ± 3	–3 ± 3	5 ± 8	8 ± 4
Tocopherol segment	0 ± 6	–6 ± 9	–2 ± 7	0 ± 11	0 ± 8
Rosiglitazone	–8 ± 3	–18 ± 3	–23 ± 3	–21 ± 6	–46 ± 11*

*Statistically significant ($P < 0.05$)

trations examined. In rosiglitazone-treated hepatocytes, reductive metabolism was comparable to controls at ≤ 500 μM, and decreased 46% at 600 μM.

Coherent multiprobe fluorescence of rat hepatocytes

This approach provided quantitative analysis of fluorescence emissions captured in every field. Control cultures showed no significant changes in membrane permeability, nuclear morphology or intracellular Ca^{2+} over the 120-min exposure period (Figs. 2, 3 and 4). Mitochondrial $\Delta\Psi_m$ decreased progressively to about 25–35% of baseline after 120 min, corresponding to a gradual loss of TMRM from hepatocytes. The concentrations tested were 200 μM and above since no effects were observed below this limit in preliminary experiments. The $\Delta\Psi_m$ profile with troglitazone at 200 μM was similar to that of control, at 300 and 400 μM $\Delta\Psi_m$ decreased 45–75% by 60 min and at 500 and 600 μM it decreased 75% from baseline in a hyperbolic function, with onset of changes within 10 min

Fig. 2 Coherent multiprobe fluorescence analysis of troglitazone-exposed rat hepatocytes. Concentration-related decreased $\Delta\Psi_m$ occurred as early as 10 min postdose at ≥300 μM. Mitochondrial changes preceded the increased plasma membrane permeability noted 40 min postdose with ≥400 μM. Nuclear condensation developed 100 min postdose at 500 and 600 μM. No effects on intracellular Ca^{2+} occurred. Each point on the different curves represents the mean of eight measurements, equivalent to the average fluorescence from a 50- to -70-cell field. The relative standard error of each sample point ranged from 5 to 20%

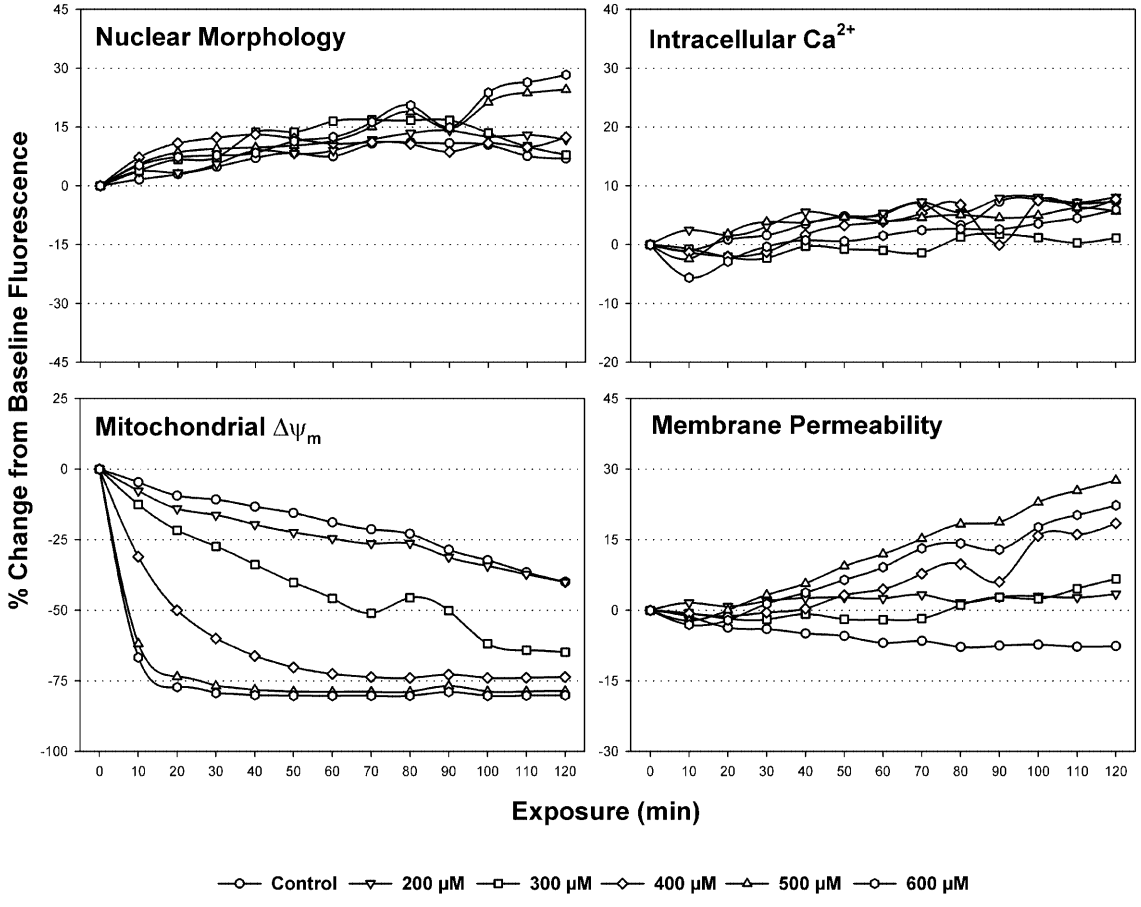

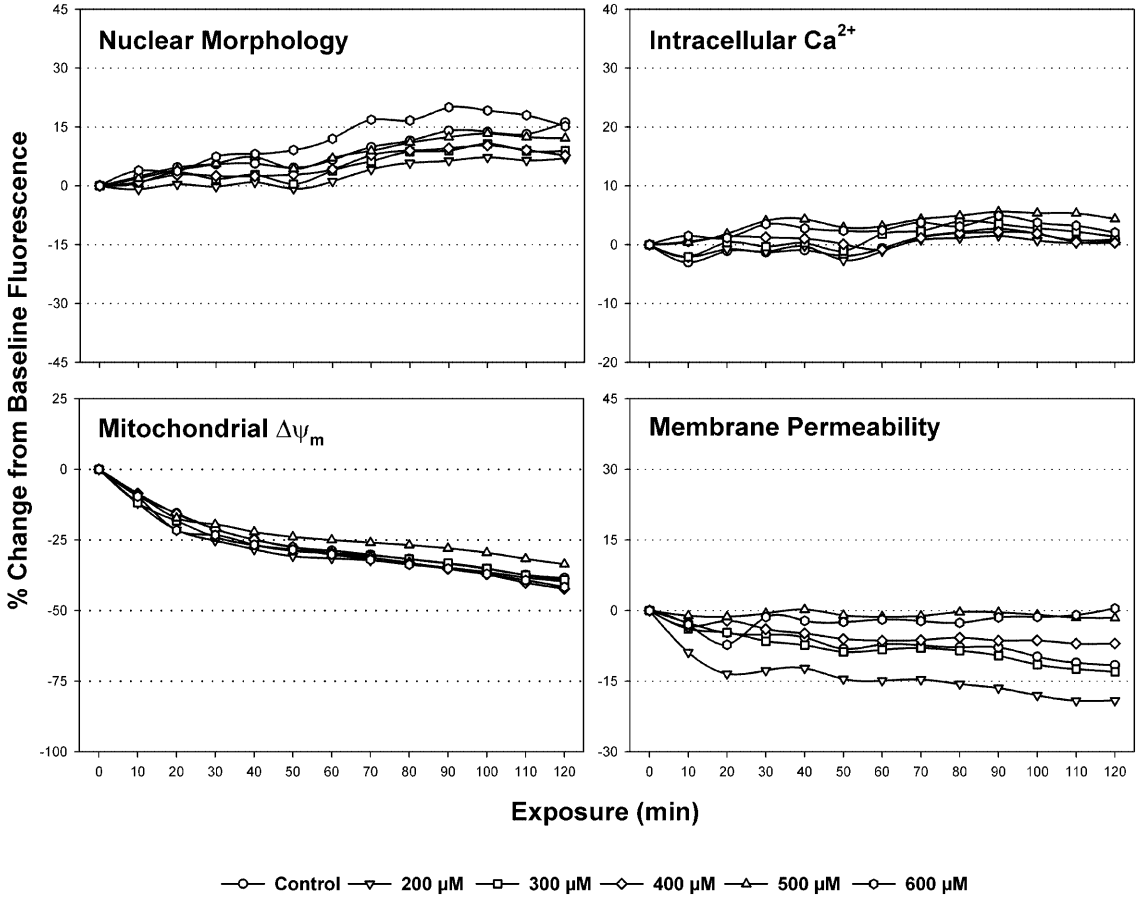

Fig. 3 Coherent multiprobe fluorescence analysis of rosiglitazone-exposed rat hepatocytes. Observed changes are small increases in nuclear condensation (indicated by increased nuclear fluorescence). Condensation was significant at 60 min postdose with 600 µM. Sampling and measurements as in Fig. 2

(Fig. 2). Membrane permeability increased after 60 min at 400, 500 and 600 µM troglitazone. Increased nuclear fluorescence, indicative of nuclear condensation, was seen after 100 minutes at 500 and 600 µM troglitazone. Cultures exposed to rosiglitazone behaved in a similar manner to controls with only a small increase in nuclear fluorescence at 60 min with 600 µM (Fig. 3). No nuclear or membrane permeability effects were seen with the troglitazone quinone (Fig. 4), and $\Delta\Psi_m$ had decreased to 50% of baseline by 120 min at 600 µM. There were no significant alterations in intracellular Ca^{2+} with any of the compounds.

The time course of morphofunctional effects was further examined by reviewing both individual and four-color composite image sequences. An example of composite images from rat hepatocytes exposed to 300 µM troglitazone is found in Fig. 5. At initiation (time zero), the field contained numerous viable hepatocytes exhibiting high $\Delta\Psi_m$ (yellow) and prominent round nuclei (blue). A few compromised cells with significant phalloidin staining (red) were visible. A loss of $\Delta\Psi_m$ was apparent in some cells by 30 min (*arrows* in Fig. 5). Continued exposure resulted in complete loss of $\Delta\Psi_m$, depletion, and eventual loss, of plasma membrane integrity. Following $\Delta\Psi_m$ depletion at 60 min, a few cells showed signs of transient increases in intracellular Ca^{2+} (green) and blebbing.

Flow cytometry of $\Delta\Psi_m$ in isolated rat hepatocytes

Troglitazone, troglitazone quinone and rosiglitazone were evaluated at equimolar concentrations from 200 to 600 µM, a range that caused overt biochemical and morphofunctional toxicity (Tables 1 and 2). Mitochondrial $\Delta\Psi_m$ did not change in hepatocytes exposed to troglitazone at 200 µM, decreased 38–64% at 300 µM by 30–60 min and decreased approximately 75% within 15 min at ≥400 µM (Fig. 6A). No significant $\Delta\Psi_m$ changes were seen with ≤ 400 µM troglitazone quinone; $\Delta\Psi_m$ decreased 21% at 500 µM by 60 min, reaching 42% at 120 min. Mitochondrial $\Delta\Psi_m$ decreased 24% by 30 min and 75% by 120 min at 600 µM (Fig. 6B). Rosiglitazone caused no significant changes in $\Delta\Psi_m$ at ≤ 500 µM; decreases of 26% occurred at 600 µM by 30 min and 55% by 60 min, remaining constant for the remaining 60 min (Fig. 6C). A summary of the 60-min IC_{50} for each compound in hepatocytes is found in Table 3.

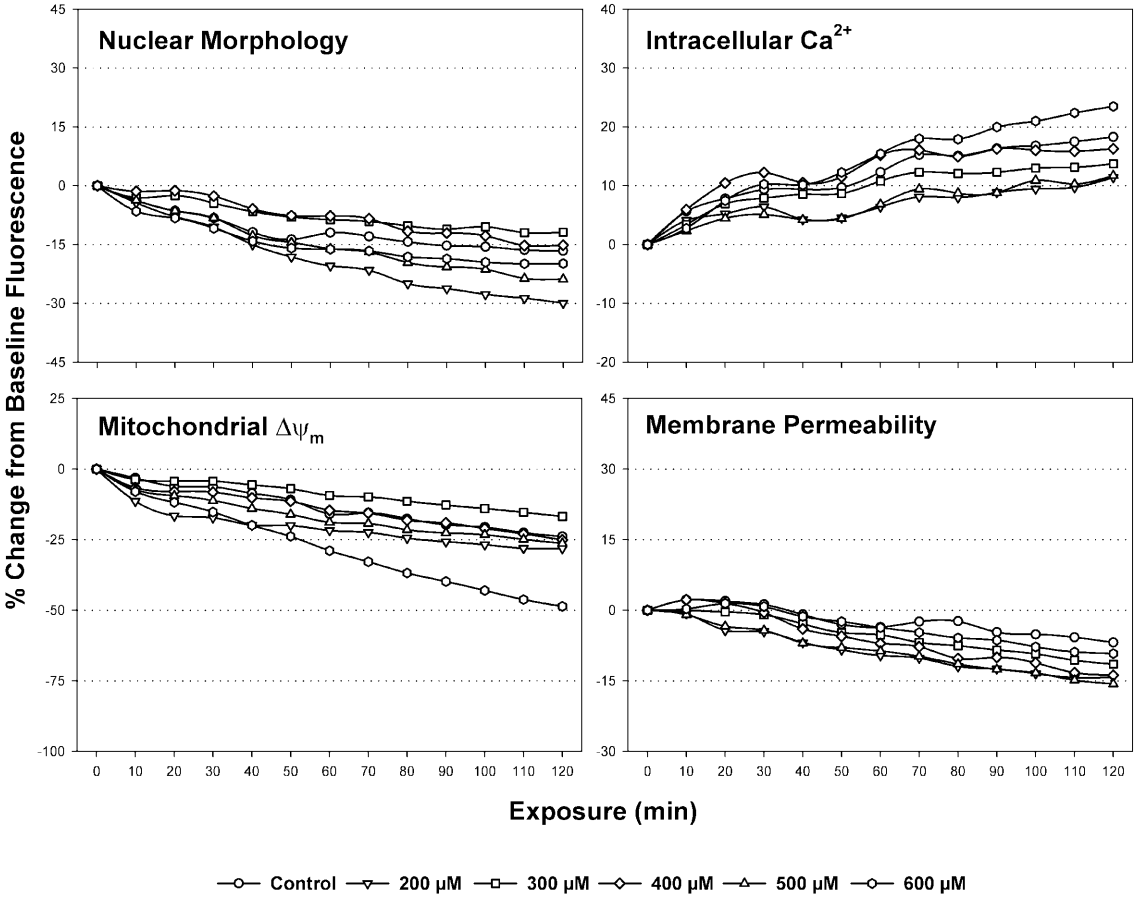

Fig. 4 Changes in coherent multiprobe fluorescence caused by troglitazone quinone metabolite in rat hepatocytes. Significant changes were decreases in $\Delta\Psi_m$ by 60 min postdose at 600 μM. No other cellular effects were seen. Sampling and measurements as in Fig. 2

ATP levels in isolated rat hepatocytes

Concentration-dependent decreases in intracellular ATP levels were observed in isolated rat hepatocytes treated with troglitazone (Fig. 7). ATP concentrations were comparable to basal levels up to 100 μM troglitazone, decreased 20%, 56% and 88% at 150, 200 and 225 μM, respectively, and there was complete (>95%) ATP depletion at 250 μM and above. With rosiglitazone, gradual decreases in intracellular ATP levels were observed at 150–500 μM and up to 95% depletion occurred between 550 and 600 μM. (Fig. 7). No significant alterations from basal ATP levels were found with 50 or 100 μM rosiglitazone.

Flow cytometry of $\Delta\Psi_m$ in isolated human hepatocytes

Mitochondrial $\Delta\Psi_m$ was monitored in normal human hepatocytes exposed to >100 μM troglitazone or rosiglitazone for 2 h (Fig. 8). The 100 μM concentration represents several multiples of the therapeutic concentration in blood and one- to two-fold of the tissue concentration of the drugs. No significant differences were found from control values at the sampled intervals. Mitochondrial $\Delta\Psi_m$ of hepatocytes from one diabetic donor showed concentration-related decreases ranging from 14 to 25% at 50 and 100 μM troglitazone (Fig. 9A). No effects were observed in the second diabetic donor or in the one exposed to rosiglitazone up to 100 μM (Fig. 9B,C).

Flow cytometry of $\Delta\Psi_m$ in isolated human PBMCs

Troglitazone, troglitazone quinone, rosiglitazone and pioglitazone were evaluated for effects on $\Delta\Psi_m$ in isolated human PBMCs. Each compound was titrated through a series of concentrations that provided minimal and maximal responses in order to determine the IC_{50} for the different cell types. Mitochondrial $\Delta\Psi_m$ was unchanged in lymphocytes at ≤ 50 μM troglitazone, decreased to 96% by 60 min at 100 μM and ≥150 μM resulted in oblated $\Delta\Psi_m$ within 15 min (Fig. 10A). Decreases of 23–77% in $\Delta\Psi_m$ were seen with 200–400 μM troglitazone quinone by 60 min, and 500–600 μM resulted in complete $\Delta\Psi_m$ depletion within 30–45 min (Fig. 10B). Lymphocyte $\Delta\Psi_m$ showed no effects with 250 μM rosiglitazone, gradually decreased by 77–82%

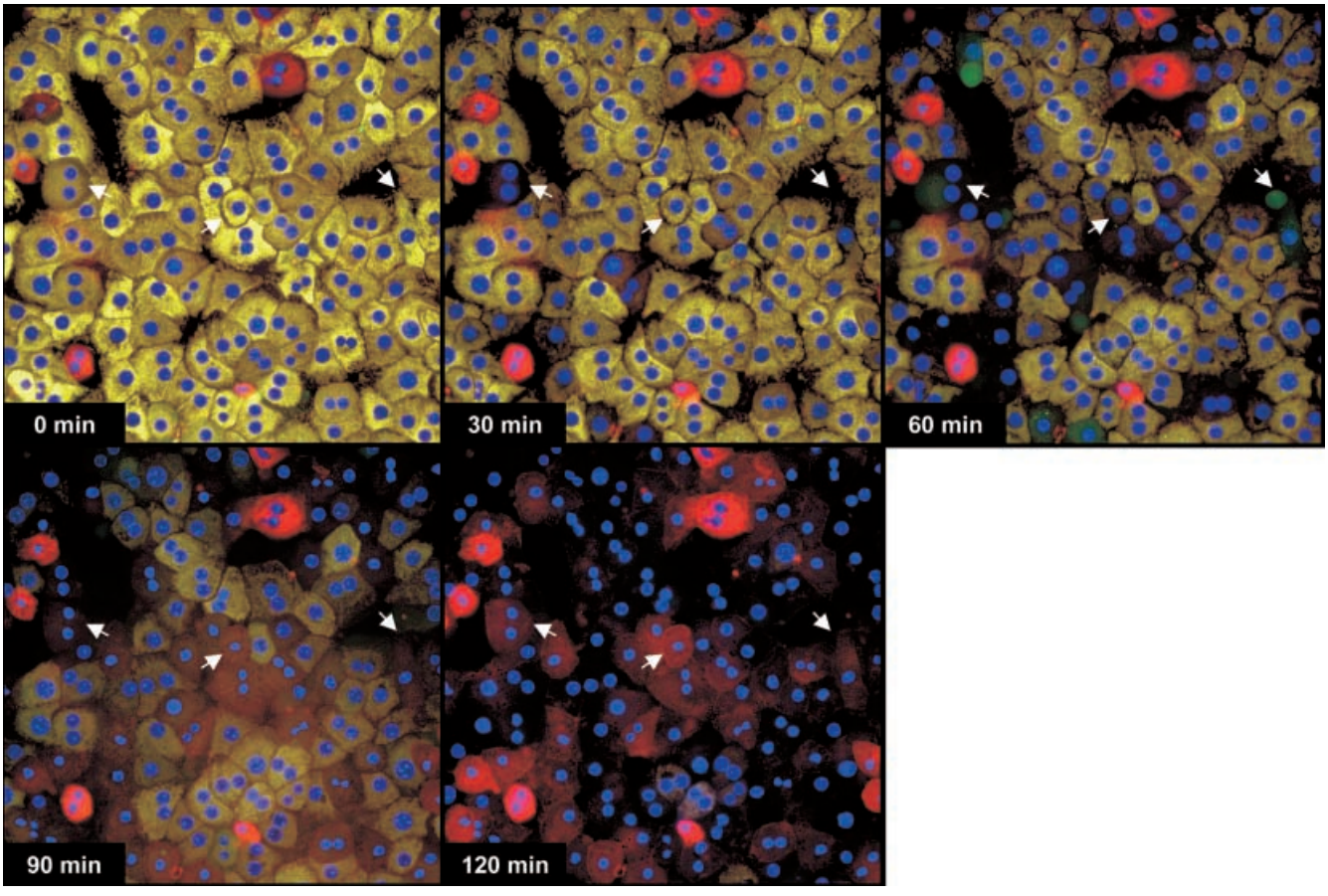

Fig. 5 Time sequence of morphofunctional changes in isolated rat hepatocytes exposed to 300 μM troglitazone. The coherent multiprobe system was designed to follow $\Delta\Psi_m$ (TMRM, *yellow*), intracellular Ca^{2+} (Fluo-4 AM,- *green*), plasma membrane permeability (Bodipy 650/665 phalloidin, *red*) and nuclear morphology (Hoechst 33342, *blue*). Numerous viable hepatocytes in *yellow* with prominent round nuclei (*blue*) and high $\Delta\Psi_m$ levels were seen at 0 min. Decreased $\Delta\Psi_m$ was noted in some cells as early as 30 min (*arrows*). Transient increases in intracellular Ca^{2+} and blebbing were seen at 60 min in a few cells. Continued troglitazone exposure (90 min, 120 min) completely depleted $\Delta\Psi_m$, and resulted in loss of plasma membrane integrity

by 60 min at 300–350 μM, and ≥450 μM resulted in complete depletion within 15 min (Fig. 10C). Mitochondrial $\Delta\Psi_m$ in lymphocytes was unchanged with ≤ 50 μM pioglitazone, and decayed by 20, 44, 76 and 98% at 100, 150, 200 and 250 μM, respectively. Pioglitazone at 300–350 μM decreased $\Delta\Psi_m$ 78–90% within 15 min and there was complete depletion by 30 min (Fig. 10D). The 60-min IC_{50} for each compound in lymphocytes is shown in Table 3.

Granulocytes had no $\Delta\Psi_m$ changes with ≤ 10 μM troglitazone; 25 and 100 μM decreased $\Delta\Psi_m$ 26–37% within 15 min and control levels were observed by 60 min. In comparison, 150 μM caused 89% decreases by 15 min and resulted in complete $\Delta\Psi_m$ depletion by 15 min at ≥200 μM (Fig. 10E). Mitochondrial $\Delta\Psi_m$ did not change with troglitazone quinone at 200 μM, decreased by 15 min at ≥300 μM and decreases reached 51, 69, and 96% at 300, 400 and 500 μM, respectively. At 600 μM, $\Delta\Psi_m$ was completely depleted by 30 min (Fig. 10F). There were no $\Delta\Psi_m$ changes with rosiglitazone at 250 μM, and ≥300 μM resulted in 15–30% lower $\Delta\Psi_m$ by 15 min, persisting to the end of the observation period (Fig. 10G). Pioglitazone at ≤ 150 μM did not change $\Delta\Psi_m$, and ≥200 μM caused 10–33% reductions by 15 min that persisted for the rest of the test (Fig. 10H). The 60-min IC_{50} for each compound in granulocytes is shown in Table 3.

Mitochondrial $\Delta\Psi_m$ in monocytes did not change with troglitazone at ≤ 25 μM, decreased 29–85% with 50–100 μM by 60 min, and complete signal loss occurred by 15 min at ≥150 μM. (Fig. 10I) The troglitazone quinone did not cause $\Delta\Psi_m$ changes at 200–300 μM, decreased $\Delta\Psi_m$ by 98% after 60 min at 400 μM, with complete depletion within 15–30 min at 500–600 μM (Fig. 10J). Rosiglitazone at 250 μM caused no changes, 300–350 μM decreased $\Delta\Psi_m$ 42–67% by 60 min, and 34–76% at ≥450 μM by 15 min with complete depletion by 60 min (Fig. 10K). Monocyte $\Delta\Psi_m$ did not change with pioglitazone at ≤ 100 μM, decreased 35% by 15 min at 150 μM was within control levels by 30 min, and at 200 μM reached 59% reduction by 60 min. Concentrations above 250 μM caused complete $\Delta\Psi_m$ depletion within 45 min (Fig. 10L). The 60-min IC_{50} for each compound in monocytes is shown in Table 3.

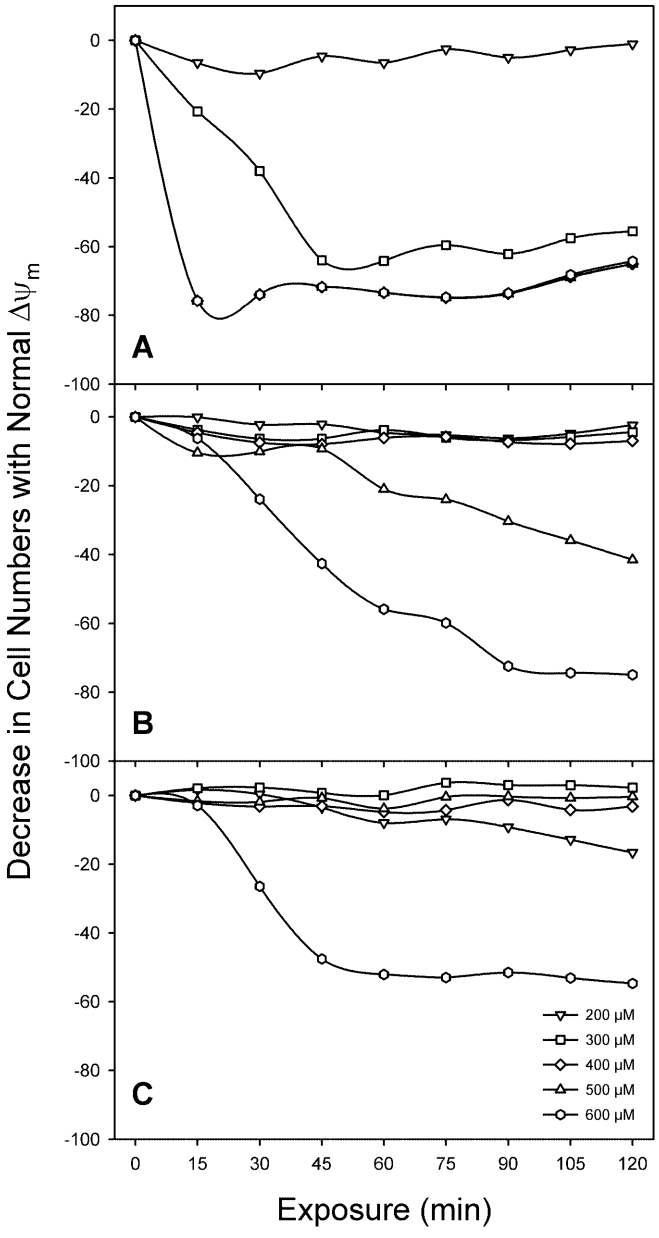

Fig. 6A–C Comparative analysis by flow cytometry of $\Delta\Psi_m$ in thiazolidinedione-exposed rat hepatocytes. Concentration-related decreases in $\Delta\Psi_m$ occurred with troglitazone (**A**), troglitazone quinone (**B**) and rosiglitazone (**C**). The 60-min IC_{50}s were 270, 584 and 591 µM for troglitazone, troglitazone quinone and rosiglitazone, respectively. Each point on the different curves represents the mean relative fluorescence distribution of 15,000 cells. The relative standard error of each gated-population ranged from 5 to 20%

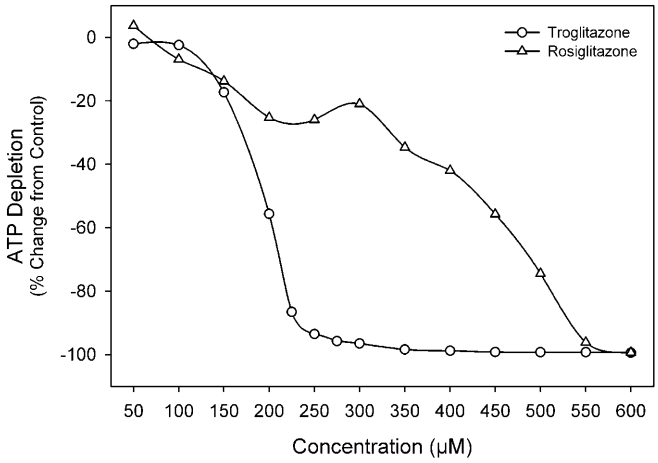

Fig. 7 Kinetics of ATP depletion in isolated rat hepatocytes after exposure to troglitazone or rosiglitazone for 2 h. Rapid depletion of ATP was observed after troglitazone at ≥150 µM, with complete depletion occurring at ≥250 µM. Gradual depletion of ATP was seen following 200–500 µM rosiglitazone, with complete depletion at 550 and 600 µM. Results indicate differences in the mechanism of nucleotide depletion. Each data point is the average of three separate experiments; the relative standard error of each sample point was < 10%

Discussion

Type II diabetes is a multifactorial disease with diverse pharmacotherapies to control glucose levels, to improve insulin production or utilization and to compensate for alterations of lipid and carbohydrate metabolic (Galloway et al. 1988; Kahn et al. 2000; National Diabetes Data Group 1985, 1987; Olefsky and Molina 1990). TZDs, in general, have similar therapeutic profiles, albeit with different relative potencies in the management of diabetics (Kameda et al. 2000; Kuehnle 1996; Oakes et al. 1994; Saltiel and Olefsky 1996; Sohda et al. 1992). TZDs are therapeutically effective in type II diabetes and more than 1.5 million diabetics are prescribed these drugs but there is insufficient information on the toxicity of this class. Although the mechanism of action is not well defined in humans, TZDs have liver cell effects that are not fully characterized and effects on cardiac muscle include glucose transport regulation and PPARγ receptor activation. Thus, the clinical effectiveness or the toxicity of these drugs may be modulated by liver or muscle involvement (Kolaczynski and Caro 1998; Reginato and Lazar 1999).

Table 3 Mitochondrial effects of thiazolidinediones on isolated rat hepatocytes and human peripheral blood mononuclear cells. Values represent the 60-min IC_{50} derived from time-response of $\Delta\Psi_m$ changes and TMRE data shown in Figs. 6 and 10. (– data not available)

Compound	IC_{50} (µM)			
	Rat hepatocytes	Human lymphocytes	Human granulocytes	Human monocytes
Troglitazone	270	83	86	81
Troglitazone quinone	584	319	303	305
Rosiglitazone	591	284	> 550	395
Pioglitazone	–	166	> 350	177

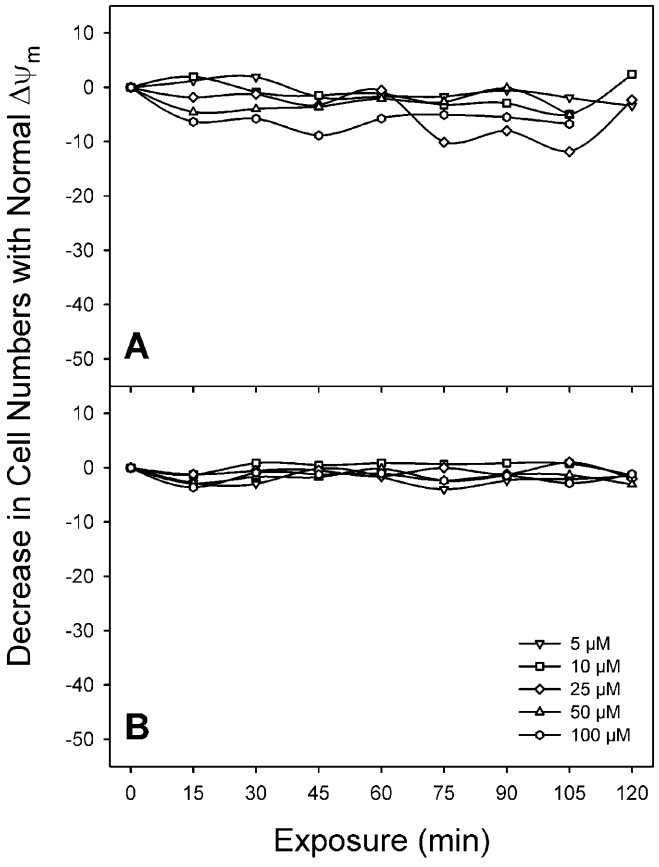

Fig. 8A, B Flow cytometric analysis of thiazolidinedione-induced changes of $\Delta\Psi_m$ in human hepatocytes from normal donors. Each panel represents a sample from an individual donor exposed to troglitazone (**A**) or rosiglitazone (**B**); each sampling point is the mean $\Delta\Psi_m$ distribution from 15,000 cells, expressed as net change from control. No significant $\Delta\Psi_m$ effects were seen in hepatocytes exposed to troglitazone or to rosiglitazone

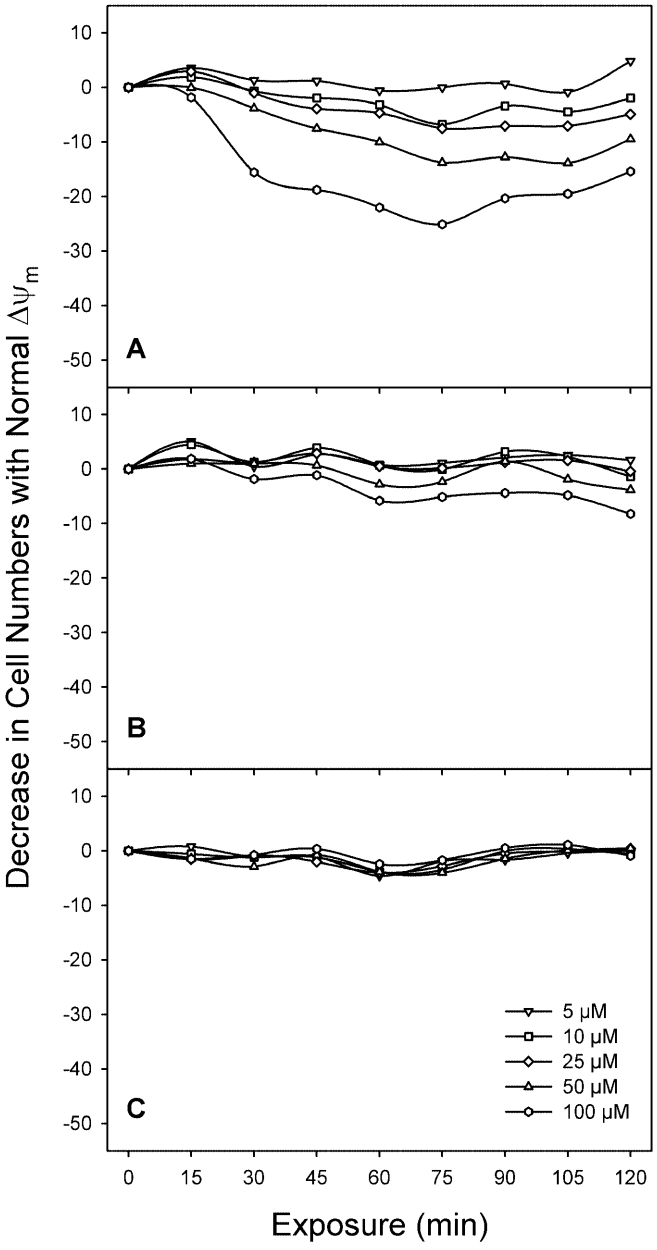

Fig. 9A–C Flow cytometric detection of changes in $\Delta\Psi_m$ in thiazolidinedione-exposed human hepatocytes from diabetic donors. Concentration-related decreases in $\Delta\Psi_m$ were seen in hepatocytes from one donor exposed to troglitazone (**A**). No mitochondrial effects were seen with a second donor (**B**) or with hepatocytes from a third donor exposed to rosiglitazone (**C**). Each panel represents an individual diabetic donor and sampling as in Fig. 8

TZDs may have hepatic injury potential since the liver is a common target of pharmacology, biotransformation and toxicity of these drugs, and serious liver damage has been reported in patients taking TZDs. Liver injury, hepatic insufficiency, hepatic transplantation or death ensued within a few weeks of troglitazone treatment. Liver injury consisted mainly of unexpected elevations of ALT and bilirubin, which in some cases were disproportionately high (Forman et al. 2000; Gitlin et al. 1998; Neuschwander-Tetri et al. 1998; Shibuya et al. 1998; Watkins and Whitcomb 1998). The liver reaction to TZDs seems unpredictable, regardless of the clinical case or patient phenotype (Fonseca et al. 1998; Iwamoto et al. 1991; Schwartz et al. 1998). Elevated aminotransferases occur sporadically in diabetics (Sherman 1991) and the enzyme elevations may result from systemic drug accumulation, metabolic overload or hypersensitivity. Further, there are no dynamic molecular or cellular mechanisms that can account for the clinical toxicity of TZDs.

The studies reported here address in vitro responses of liver cells to TZDs under real-time conditions in order to understand the toxicity caused by these drugs. Most approaches to in vitro cellular toxicity monitor single parameters in live or fixed cells (de la Iglesia et al. 1999; Plymale and de la Iglesia 1999). Recently, because of advances in fluorescence technology, it became possible to monitor simultaneous intracellular events and to dissect pathways leading to cell dysfunction, injury and death. Coherent multiprobe fluorescence microscopy provides sequential analyses of intracellular

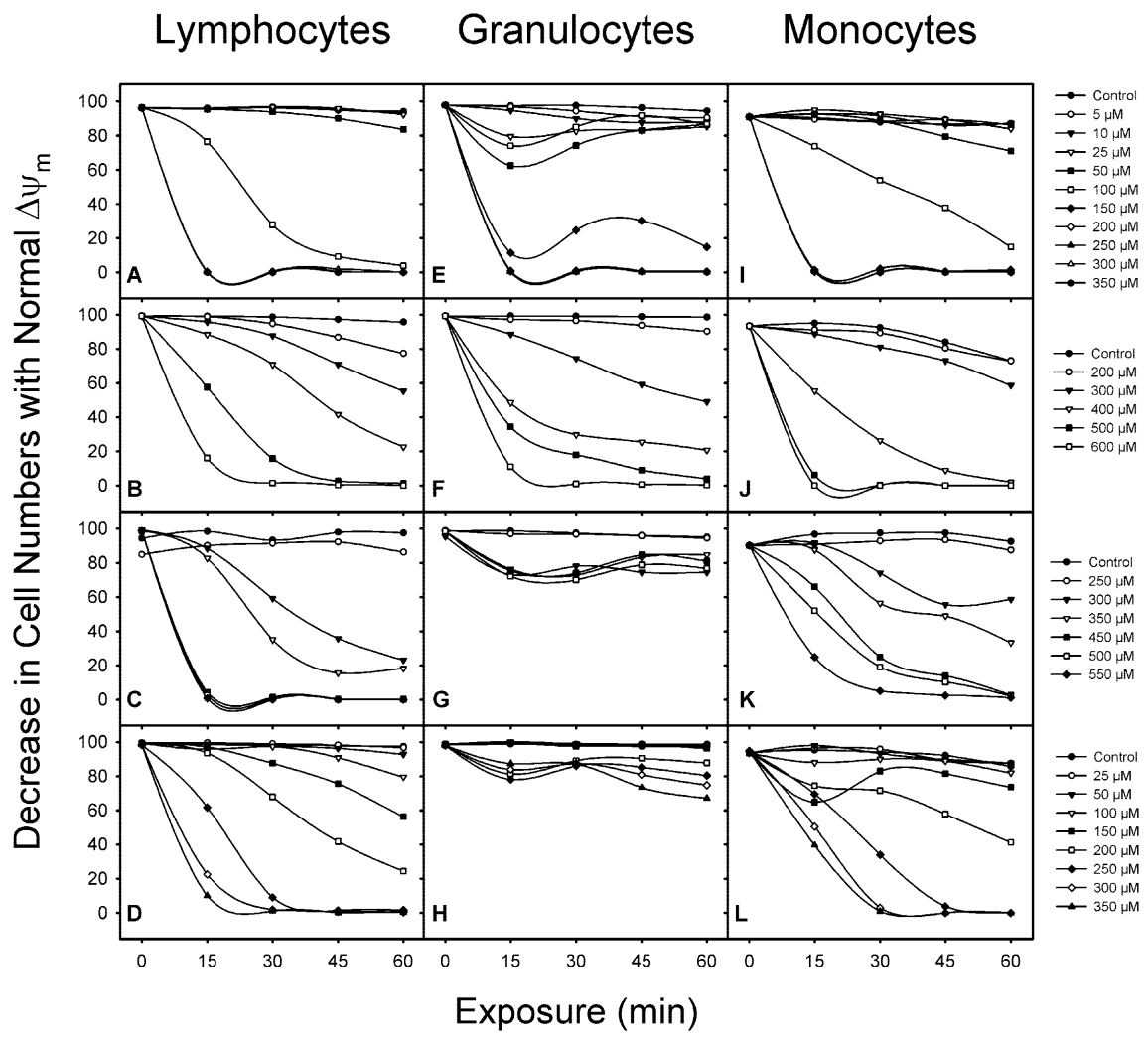

Fig. 10 Comparison of $\Delta\Psi_m$ changes in thiazolidinedione-exposed human peripheral blood mononuclear cells by flow cytometry. Concentration-related decreases in $\Delta\Psi_m$ were seen with troglitazone (**A,E,I**) and troglitazone quinone (**B,F,J**). For lymphocytes, granulocytes and monocytes, the 60-min IC_{50}s ranged from 81 to 86 μM with troglitazone and between 303 and 319 μM with troglitazone quinone. Variable responses were seen in cells exposed to rosiglitazone (**C,G,K**) and pioglitazone (**D,H,L**). Respective IC_{50}s were 284 and 166 μM in lymphocytes (**C,D**) and 395 and 177 μM in monocytes (**K,L**). Granulocytes were more resistant with IC_{50} of >350 and >550 μM for pioglitazone (**H**) and rosiglitazone (**G**), respectively. Each data point represents the average measurement from four individual normal donors; the relative standard error for each sample point was $<10\%$

activities on a near real-time basis (Plymale et al. 1999) and uses specific functional fluorescent probes that are coordinated in kinetic assays to reveal phenomena that otherwise are not observable in single time-point assays with fixed or disrupted cells. The effects of tacrine, a drug that consistently caused increased liver transaminases in Alzheimer's patients, were characterized in human and animal hepatocytes with a three-probe assay ; (Plymale et al. 1999; Watkins et al. 1994). Mitochondrial $\Delta\Psi_m$ was followed with tetramethylrhodamine, a sensitive indicator of mitochondrial function (Lemasters et al. 1998; Lemasters et al. 1999). The decreased mitochondrial potential correlated with uncoupling of oxidative phosphorylation in isolated mitochondria (Monteith et al. 1998; Plymale and de la Iglesia 1999; Plymale et al. 1999). Plasma membrane integrity and cytoskeletal changes were monitored using conjugated phalloidin, a large molecular weight fluorescent probe that remains in the media and covalently binds to F-actin monomers and fluoresces after entering the cell. Fluo-4 AM is an indicator of cytoplasmic Ca^{2+} trafficking and nuclear morphology was followed using Hoescht 33342. The coherent use of these probes and spectral filters enabled the systematic monitoring of fluorescence changes on a quantitative basis. A panel of four probes was used to define the time course of intracellular events with TZDs.

Troglitazone above 200 μM decreased $\Delta\Psi_m$ initially with increased plasma membrane permeability, and Ca^{2+} influx was seen later. A series of assays for subcellular damage by different functional groups of the troglitazone molecule or metabolites showed no significant effects. The lack of effects by metabolites or functional groups and the sudden fall in intracellular ATP levels induced by troglitazone, suggest a rapid-onset and

direct action. Microsomal incubations yielded the formation of oxidative scission products that were attributed a role in the toxicity mechanism (Kassahun et al. 2001). Although the potential for toxicity exists, there are no available in-life studies that could corroborate these postulates. The oxidative metabolite formation is NADPH-dependent, and the role of such system in ATP-depleted and uncoupled intact liver cells has not been studied. Rosiglitazone decreased $\Delta\Psi_m$ less than troglitazone, and both drugs caused a fall in intracellular ATP. Thus, the $\Delta\Psi_m$ changes revealed unsuspected differences and similarities between TZDs in liver cells that present an opportunity for further investigations. The early effects on mitochondrial energetics are due to irreversible uncoupling of oxidative phosphorylation. The toxicity of troglitazone has been attributed to the formation of a reactive quinone metabolite (Elcock et al. 1999) and to a quinone methide conjugate (Kassahun et al. 2001). It is not known to what extent the liver cell can compensate or neutralize the oxidative damage from these compounds. The early onset of mitochondrial uncoupling and transmembrane potential loss caused by TZDs precede the appearance of metabolic biotransformation products that are detected in the bile. Multiprobe fluorescence showed minimal $\Delta\Psi_m$ changes were induced by the quinone metabolite, with lesser or no effects on other cell functions. The ALT leakage was of borderline significance and was corroborated by the lack of increased plasma membrane permeability. The $\Delta\Psi_m$ changes may explain the attenuation of effects by either troglitazone or the uncoupler carbonyl cyanide *m*-chlorophenylhydrazone (CCCP) on mitochondria from Zucker diabetic female rats (Haskins et al. 1999). Zucker diabetic rats have a pre-existing decreased $\Delta\Psi_m$, and reduction of mitochondrial superoxide production controls hyperglycemic damage, an inherently beneficial paradox (Nishikawa et al. 2000). Diabetic mitochondria had no further decreases in $\Delta\Psi_m$ after troglitazone, but the overall transmembrane potential remained lower than controls.

The effects of troglitazone and rosiglitazone on cryopreserved hepatocytes from normal or diabetic humans were explored and the samples showed the range of mitochondrial changes in diabetic livers. Since cryopreservation may have affected some sensitive energy-dependent functions, data from freshly isolated liver cells exposed to TZDs would be useful to confirm our results. Troglitazone-related $\Delta\Psi_m$ changes in human diabetic hepatocytes were comparable to those in normal rat liver cells, suggesting similar mechanisms of injury at the cellular level in humans and rats. Peroxidative damage to mitochondria may contribute to the development of diabetic complication (Nishikawa et al. 2000) but data are lacking to compare $\Delta\Psi_m$ from diabetic animals receiving TZDs.

While studying the mechanism of TZD-mediated hepatocyte injury, it was desirable to develop a marker of cellular effects that would be applicable to the clinical setting. Animal studies did not reveal clinical or pathological evidence of liver changes in troglitazone long-term studies, as opposed to the short-term onset of hepatotoxicity in humans. Rodents and monkeys metabolize troglitazone in a similar manner to humans and were given large daily doses in chronic studies without signs of clinical liver reactions or microscopic liver injury (Herman et al. 1997; McGuire et al. 1997; Rothwell et al. 1997). Changes in $\Delta\Psi_m$, however, are characteristically reproducible across species with quantitative differences being a function of species-specific compensatory mechanisms. It is only recently that the mitochondrial transmembrane potential appears as an early and sensitive indicator of damage, is accompanied by ATP depletion and is followed by increased membrane permeability. Future studies should address the downstream effects of these changes, since nuclear condensation and apoptosis are observed as late effects that are shared by TZDs.

Functional mitochondrial markers in serially sampled cultures of human PBMCs exposed to TZDs mimicked the effects seen in human or animal liver cells by flow cytometry. Mitochondrial $\Delta\Psi_m$ changes were consistently reproducible in rapid and simple assays in discrete white blood cell populations with the IC_{50} as a sensitive index. Thus, flow cytometry represents a practical and easily available technology that many laboratories could apply to monitor cellular effects of potential toxicants. We propose that monitoring the early toxicity indicator $\Delta\Psi_m$ in white blood cells should become available to diabetics in order to anticipate or prevent adverse hepatic reactions.

References

Cabarrou A, Laguens R, Caino H, Doria I, Auciello N, Cedola N, Ponce de Leon H (1973) The diabetic liver. Cytochemical, ultrastructural, and enzymatic changes. Acta Diabetol Lat 10:1236–1268

Davies GF, Khandelwal RL, Roesler WJ (1999a) Troglitazone induces expression of PPARγ in liver. Mol Cell Biol Res Commun 2: 202–208

Davies GF, Khandelwal RL, Roesler WJ (1999b) Troglitazone inhibits expression of the phosphoenolpyruvate carboxykinase gene by an insulin-independent mechanism. Biochim Biophys Acta 1451:122–131

de la Iglesia FA, Herman JR, McGuire EJ, Gough AW, Masuda H (1998) Chronic toxicity study of the antidiabetic troglitazone in Wistar rats. Toxicol Sci 42:50 (Abstr 246)

de la Iglesia FA, Robertson DG, Haskins JR (1999) Morphofunctional aspects of the hepatic architecture: functional and subcellular correlates. In: Woolf TF (ed) Handbook of drug metabolism. Marcel Dekker, New York, pp 81–107

Deschenes J, Valet JP, Marceau N (1980) Hepatocytes from newborn and weanling rats in monolayer culture: isolation by perfusion, fibronectin-mediated adhesion, spreading, and functional activities. In Vitro 16:722–730

Elcock FJ, Lyon JJ, Hitchcock JM, Molton SA, Morgan DG, Bertram TA, Bugelski PJ (1999) Toxicity of troglitazone in cultures rat hepatocytes (Abstr). Diabetes 48:A63

Fonseca VA, Valiquett TR, Huang SM, Ghazzi MN, Whitcomb RW (1998) Troglitazone monotherapy improves glycemic control in patients with type 2 diabetes mellitus: a randomized, controlled study. The Troglitazone Study Group. J Clin Endocrinol Metab 83:3169–3176

Forman LM, Simmons DA, Diamond RH (2000) Hepatic failure in a patient taking rosiglitazone. Ann Intern Med 132:118–121

Fujiwara T, Yoshioka S, Yoshioka T, Ushiyama I, Horikoshi H (1988) Characterization of new oral antidiabetic agent CS-045. Studies in KK and ob/ob mice and Zucker fatty rats. Diabetes 37:1549–1558

Galloway J, Potvin J, Schuman C (1988) Diabetes mellitus, 9th edn. Eli Lilly & Co., Indianapolis

Gitlin N, Julie NL, Spurr CL, Lim KN, Juarbe HM (1998) Two cases of severe clinical and histologic hepatotoxicity associated with troglitazone. Ann Intern Med 129:36–38

Haskins JR, Johnson JH, de la Iglesia FA (1999) Ex vivo functional assessment of mitochondrial transmembrane potential from lean and diabetic Zucker rats with or without troglitazone (Abstr). Diabetes 48:A262

Herman JR, Metz AL, McGuire EJ, de la Iglesia FA, Masuda H (1997) Subchronic toxicity of the antidiabetic troglitazone in Wistar rats (Abstr). Toxicologist 36:273

Herman JR, McGuire EJ, de la Iglesia FA, Walsh KM, Masuda H (1998) Carcinogenicity study of the antidiabetic troglitazone in Wistar rats (Abstr). Toxicol Sci 42:71

Ihara H, Urano T, Takada A, Loskutoff DJ (2001) Induction of plasminogen activator inhibitor-1 (PAI-1) gene expression in adipocytes by thiazolidinediones. FASEB J 15:1233–1235. DOI 10:.1096/fj.00–0570fje

Iwamoto Y, Kuzuya T, Matsuda A, Awata T, Kumakura S, Inooka G, Shiraishi I (1991) Effect of new oral antidiabetic agent CS-045 on glucose tolerance and insulin secretion in patients with NIDDM. Diabetes Care 14:1083–1086

Kahn CR, Chen L, Cohen SE (2000) Unraveling the mechanism of action of thiazolidinediones. J Clin Invest 106:1305–1307

Kameda N, Okuya S, Oka Y (2000) Rosiglitazone (BRL-49653). Nippon Rinsho 58:401–404

Kassahun K, Pearson PG, Tang W, McIntosh I, Leung K, Elmore C, Dean D, Wang R, Doss G, Baillie TA (2001) Studies on the metabolism of troglitazone to reactive intermediates in vitro and in vivo. Evidence for novel biotransformation pathways involving quinone methide formation and thiazolidinedione ring scission. Chem Res Toxicol 14:62–70

Kawai K, Kawasaki-Tokui Y, Odaka T, Tsuruta F, Kazui M, Iwabuchi H, Nakamura T, Kinoshita T, Ikeda T, Yoshioka T, Komai T, Nakamura K (1997) Disposition and metabolism of the new oral antidiabetic drug troglitazone in rats, mice and dogs. Arzneimittelforschung 47:356–368

Kolaczynski JW, Caro JF (1998) Insulin resistance: site of the primary defect or how the current and the emerging therapies work. J Basic Clin Physiol Pharmacol 9:281–294

Kostrubsky VE, Sinclair JF, Ramachandran V, Venkataramanan R, Wen YH, Kindt E, Galchev V, Rose K, Sinz M, Strom SC (2000) The role of conjugation in hepatotoxicity of troglitazone in human and porcine hepatocyte cultures. Drug Metab Dispos 28:1192–1197

Kuehnle HF (1996) New therapeutic agents for the treatment of NIDDM. Exp Clin Endocrinol Diabetes 104:93–101

Lehmann JM, Moore LB, Smith-Oliver TA, Wilkison WO, Willson TM, Kliewer SA (1995) An antidiabetic thiazolidinedione is a high affinity ligand for peroxisome proliferator-activated receptor γ (PPAR γ). J Biol Chem 270:12953–12956

Lemasters JJ, Nieminen AL, Qian T, Trost LC, Elmore SP, Nishimura Y, Crowe RA, Cascio WE, Bradham CA, Brenner DA, Herman B (1998) The mitochondrial permeability transition in cell death: a common mechanism in necrosis, apoptosis and autophagy. Biochim Biophys Acta 1366:177–196

Lemasters JJ, Qian T, Bradham CA, Brenner DA, Cascio WE, Trost LC, Nishimura Y, Nieminen AL, Herman B (1999) Mitochondrial dysfunction in the pathogenesis of necrotic and apoptotic cell death. J Bioenerg Biomembr 31:305–319

Lowis EI, Oakey RE (1996) Steroid sulphatase deficiency: identification of heterozygotes using hydrolysis of dehydroepiandrosterone sulphate by peripheral leucocytes. Ann Clin Biochem 33:219–226

McGuire EJ, Dethloff LA, Walsh KM, de la Iglesia FA, Masuda H (1997) Subchronic toxicity of the antidiabetic troglitazone in B6C3F1 mice. Toxicologist 36:273 (Abstr 1388)

McGuire EJ, Dethloff LA, Parker RF, de la Iglesia FA, Gough AW, Masuda H (1998) Carcinogenicity study of the antidiabetic troglitazone in B6C3F1 mice. Toxicol Sci 42:50 (Abstr 247)

Monteith DK, Theiss JC, Haskins JR, de la Iglesia FA (1998) Functional and subcellular organelle changes in isolated rat and human hepatocytes induced by tetrahydroaminoacridine. Arch Toxicol 72:147–156

Murakami T, Shima K (1995) Diabetogenes; which cause type II diabetes mellitus. Rinsho Byori 43:781–785

National Diabetes Data Group (1985) Diabetes in America. US Department of Health and Human Services. National Institutes of Health: Publ No 85-1468

National Diabetes Data Group (1987) Noninsulin-dependent diabetes. US Department of Health and Human Services. National Institutes of Health: Publ No 87-241

Neuschwander-Tetri BA, Isley WL, Oki JC, Ramrakhiani S, Quiason SG, Phillips NJ, Brunt EM (1998) Troglitazone-induced hepatic failure leading to liver transplantation. A case report. Ann Intern Med 129: 38–41

Nishikawa T, Edelstein D, Du XL, Yamagishi S, Matsumura T, Kaneda Y, Yorek MA, Beebe D, Oates PJ, Hammes HP, Giardino I, Brownlee M (2000) Normalizing mitochondrial superoxide production blocks three pathways of hyperglycaemic damage. Nature 404:787–490

Oakes ND, Kennedy CJ, Jenkins AB, Laybutt DR, Chisholm DJ, Kraegen EW (1994) A new antidiabetic agent, BRL 49653, reduces lipid availability and improves insulin action and glucoregulation in the rat. Diabetes 43:1203–1210

Olefsky J, Molina J (1990) Insulin resistance in man. In: Rifkin H, Porte DJ (eds) Diabetes mellitus theory and practice, 4th edn. Elsevier, New York, pp 121–153

Ott P, Ranek L, Young MA (1998) Pharmacokinetics of troglitazone, a PPAR-γ agonist, in patients with hepatic insufficiency. Eur J Clin Pharmacol 54:567–571

Plymale DR, de la Iglesia FA (1999) Acridine-induced subcellular and functional changes in isolated human hepatocytes in vitro. J Appl Toxicol 19:31–38

Plymale DR, Haskins JR, de la Iglesia FA (1999) Monitoring simultaneous subcellular events in vitro by means of coherent multiprobe fluorescence. Nat Med 5:351–355

Ramachandran V, Kostrubsky VE, Komoroski BJ, Zhang S, Dorko K, Esplen JE, Strom SC, Venkataramanan R (1999) Troglitazone increases cytochrome P-450 3 A protein and activity in primary cultures of human hepatocytes. Drug Metab Dispos 27:1194–1199

Reginato MJ, Lazar MA (1999) Mechanisms by which thiazolidinediones enhance insulin action. Trends Endocrinol Metab 10:9–13

Rothwell CE, Bleavins MR, McGuire EJ, de la Iglesia FA, Masuda H (1997) 52-Week oral toxicity study of troglitazone in cynomolgus monkeys (Abstr). Toxicologist 36:273

Saltiel AR, Olefsky JM (1996) Thiazolidinediones in the treatment of insulin resistance and type II diabetes. Diabetes 45:1661–1669

Schwartz S, Raskin P, Fonseca V, Graveline JF (1998) Effect of troglitazone in insulin-treated patients with type II diabetes mellitus. Troglitazone and exogenous insulin Study Group. N Engl J Med 338:861–866

Seglen PO (1976) Preparation of isolated rat liver cells. Methods Cell Biol 13:29–83

Sherman KE (1991) Alanine aminotransferase in clinical practice. A review. Arch Intern Med 151:260–265

Shibukawa A, Sawada T, Nakao C, Izumi T, Nakagawa T (1995) High-performance frontal analysis for the study of protein binding of troglitazone (CS-045) in albumin solution and in human plasma. J Chromatogr A 697:337–343

Shibuya A, Watanabe M, Fujita Y, Saigenji K, Kuwao S, Takahashi H, Takeuchi H (1998) An autopsy case of troglitazone-induced fulminant hepatitis. Diabetes Care 21:2140–243

Silverman JF, Pories WJ, Caro JF (1989) Liver pathology in diabetes mellitus and morbid obesity. Clinical, pathological, and biochemical considerations. Pathol Annu 24:275–302

Sohda T, Mizuno K, Momose Y, Ikeda H, Fujita T, Meguro K (1992) Studies on antidiabetic agents. 11. Novel thiazolidinedione derivatives as potent hypoglycemic and hypolipidemic agents. J Med Chem 35:2617–2626

Tattersall R (1995) Traditional pharmacological management of non-insulin-dependent diabetes. Clin Invest Med 18:288–295

Watkins PB, Whitcomb RW (1998) Hepatic dysfunction associated with troglitazone. N Engl J Med 338: 916–917

Watkins PB, Zimmerman HJ, Knapp MJ, Gracon SI, Lewis KW (1994) Hepatotoxic effects of tacrine administration in patients with Alzheimer's disease. JAMA 271: 992–998